ELSEVIER

Journal of Power Sources 99 (2001) 66–69

JOURNAL OF POWER SOURCES

www.elsevier.com/locate/jpowsour

Electrochemical insertion of magnesium to $Mg_{0.5}Ti_2(PO_4)_3$

Koji Makino*, Yasushi Katayama, Takashi Miura, Tomiya Kishi

Department of Applied Chemistry, Faculty of Science and Technology, Keio University, Hiyoshi 3-14-1, Kohoku-ku, Yokohama 223-8522, Japan

Received 25 August 2000; received in revised form 11 October 2000; accepted 20 December 2000

Abstract

$Mg_{0.5}Ti_2(PO_4)_3$ having NASICON-lattice was prepared by sol–gel method and evaluated as a cathode material for magnesium cells. The crystalline phase could be successfully obtained after heating at 600°C. Electrochemical magnesium insertion from a propylene carbonate solution into this host was found possible and one Mg^{2+} ion could be accommodated per unit formula. However, the magnesium insertion process was under kinetic control of Mg^{2+} diffusion due to the low mobility of Mg^{2+} in this host. © 2001 Elsevier Science B.V. All rights reserved.

Keywords: Magnesium battery; Magnesium titanium phosphate; Electrochemical magnesium insertion

1. Introduction

Magnesium cells may be a candidate of high energy density cells competable with lithium cells, because the raw material costs may be lower than those in lithium cells and magnesium is less dangerous than lithium. However, it is so far well known that Mg^{2+} insertion into ion-transfer hosts proceeds slowly owing to the strong polarization effect of small and divalent Mg^{2+} ion compared with Li^+ or Na^+ and only a small discharge capacity has been reported for magnesium insertion cathode [1–5]. Consequently, it is necessary to realize fast Mg^{2+} transport in the host in addition to other requirements as practical cathode materials for magnesium cells.

Both lithium and sodium ions can be inserted/extracted reversibly into/from a series of compounds having a general formula of $A_nM_2(XO_4)_3$ (A = Li or Na; M = transition metal; X = S, P or As) [6–8], derived from well-known fast ionic conductor of NASICON [9], because they have large enough interstitial voids to uptake guest species and high structural stability based on three-dimensional framework. Similarly, fast Mg^{2+} transport may also be expected in such compound lattice, which seems as promising host for magnesium.

In this study, NASICON-structured $Mg_{0.5}Ti_2(PO_4)_3$ samples were prepared by sol–gel method and investigated electrochemically as a magnesium host.

2. Experimental

2.1. Preparation of $Mg_{0.5}Ti_2(PO_4)_3$

0.1 mol dm^{-3} $Mg(CH_3COO)_2{\cdot}4H_2O$ (Wako Chemical, >99%) and 0.1 mol dm^{-3} $NH_4H_2PO_4$ (Wako Chemical, >99%) aqueous solutions were prepared separately, in addition to 0.1 mol dm^{-3} $C_4H_9O[Ti(OC_4H_9)_2O]_4C_4H_9$ (Wako Chemical, >95%) ethanol solution. These solutions were mixed at the stoichiometric ratio to give $Mg_{0.5}Ti_2(PO_4)_3$. The obtained sol solution was further stirred at 70°C for 6 h to form a gel, which was then dried at 90°C for 12 h to give a powder. The powder was heated at 300 and then 500°C to remove ammonium and acetate groups, followed by final firing at various temperatures for 24 h.

2.2. Electrochemical measurements

Electrochemical magnesium insertion from 1 mol dm^{-3} $Mg(ClO_4)_2$/propylene carbonate (PC) solution was performed in a cylindrical glass cell. The sample electrode pellet was prepared by pressing the 70:25:5 (in wt.) mixture of $Mg_{0.5}Ti_2(PO_4)_3$, acetylene black (Denka Black) and PTFE (Mitsui-Du Pont) at a pressure of 2×10^3 kg cm^{-2} onto a porous nickel sheet. Magnesium ribbon was used as the counter electrode. The reference electrode consisted of a silver wire immersed in 0.1 mol dm^{-3} $AgClO_4$/PC solution, which was separated from the cell electrolyte by a glass filter. Similarly, electrochemical lithium insertion from 1 mol dm^{-3} $LiClO_4$/PC solution was performed with the lithium wire counter electrode. All procedures and cell

* Corresponding author.

PII: S0378-7753(01)00480-3

construction were carried out under dried argon atmosphere in a grove box.

X-ray diffraction (XRD, Rigaku, RINT-1300) measurements were performed on a nickel substrate both before and after electrochemical measurements as well as for prepared $Mg_{0.5}Ti_2(PO_4)_3$ powder on a glass plate.

3. Results and discussion

3.1. Preparation of $Mg_{0.5}Ti_2(PO_4)_3$

$Mg_{0.5}Ti_2(PO_4)_3$ finally fired below 500°C showed amorphous XRD pattern as in Fig. 1. $Mg_{0.5}Ti_2(PO_4)_3$ finally fired at 600°C, on the other hand, gave a set of XRD peaks which could be assigned for the hexagonal lattice (space group $R\bar{3}c$). This phase has so far been obtained at 766°C by Barth et al. [10] or at 700–750°C by Miyamoto et al. [11]. The formation of $Mg_{0.5}Ti_2(PO_4)_3$ phase at 600°C may be explained by different starting materials and a slow heating rate of 0.2°C min^{-1}. Moreover, the unit cell parameters of $a = 0.852$ nm and $c = 2.10$ nm are independent of final firing temperatures between 600 and 900°C.

3.2. Electrochemical magnesium insertion

Galvanostatic discharge curves at $-50\ \mu A\ cm^{-2}$ for $Mg_{0.5}Ti_2(PO_4)_3$ finally fired at 700°C are compared in Fig. 2 in order to optimize the [active material]/[acetylene black] ratio (r), since NASICON-structured compounds have low electronic conductivities in general. For $r = 70/25$, the potential plateau at about -1.6 V (versus Ag^+/Ag) continues until the limit of one-electron accommodation by Ti^{4+}/Ti^{3+} (reduction of Ti^{4+} to Ti^{3+}) defined as $x = 1$, where x denotes the calculated amount of inserted Mg^{2+} per unit formula. At the discharge potential below -2.4 V, an unexpected reaction such as solvent decomposition might occur. On the other hand, for $r = 90/5$, a large potential drop

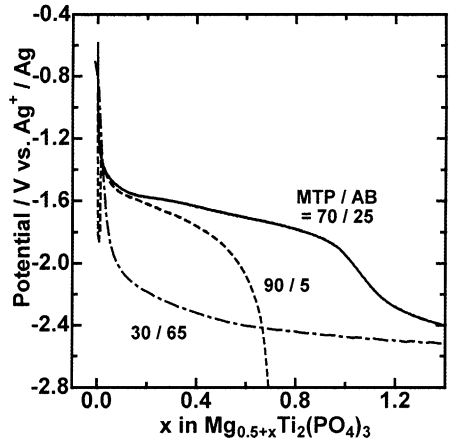

Fig. 2. Galvanostaic ($-50\ \mu A\ cm^{-2}$) discharge curves for different [$Mg_{0.5}Ti_2(PO_4)_3$]/[acetylene black] ratios.

on initial discharge is a characteristic of low electronic conductivity and the extent of Mg^{2+} insertion is limited to about $x = 0.6$. For $r = 30/65$, the potential plateau at -1.6 V disappears completely and the potential approaches to the -2.4 V region immediately. These results may suggest that the electronic conduction paths are not enough in the electrode at $r = 90/5$, whereas the ionic conduction paths are blocked by too much carbon at $r = 30/65$. Further investigations were carried out by employing the appropriate $r = 70/25$ sample electrodes.

Galvanostatic discharge curves at various current densities per apparent geometrical area are compared in Fig. 3. The plateau becomes the shorter and lower at the higher current density, owing to the low mobility of Mg^{2+} in the host lattice. In order to confirm the diffusion-controlled situation in the host matrix, the limiting amount of Mg insertion, (x_{lim}) which corresponds to plateau length until about -2.2 V, is determined from the inflection point of discharge curves at various current densities (j). As seen in Fig. 4, there can be found a proportional relation between

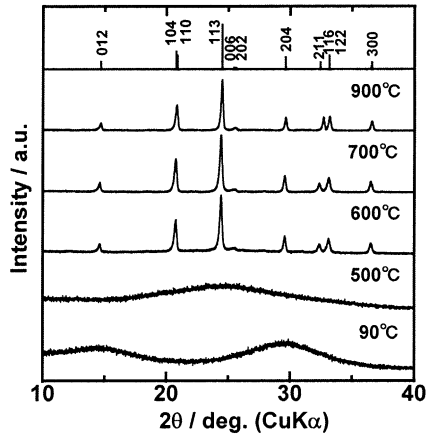

Fig. 1. XRD patterns of $Mg_{0.5}Ti_2(PO_4)_3$ obtained at various firing temperatures. Simulation: space group $R\bar{3}c$, $a = 0.852$ nm, $c = 2.10$ nm.

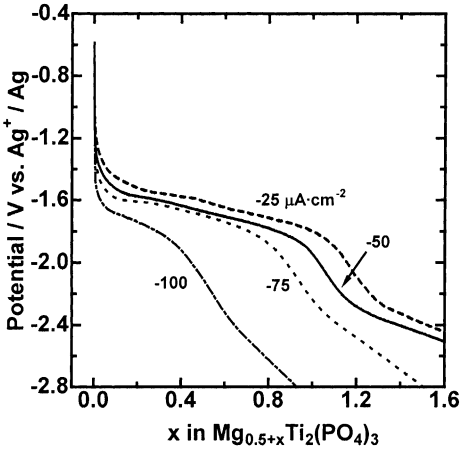

Fig. 3. Discharge curves of $Mg_{0.5}Ti_2(PO_4)_3$ at various current densities.

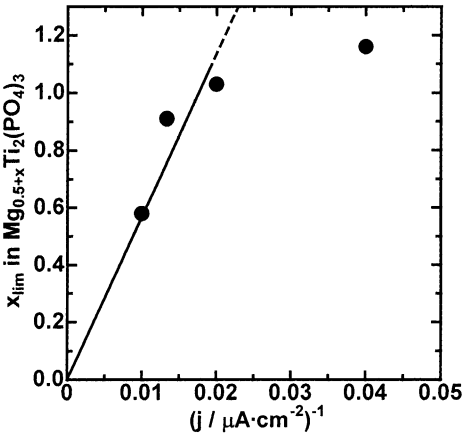

Fig. 4. Relationship between the limit of Mg insertion x_{lim} in $Mg_{0.5+x}Ti_2(PO_4)_3$ and current density.

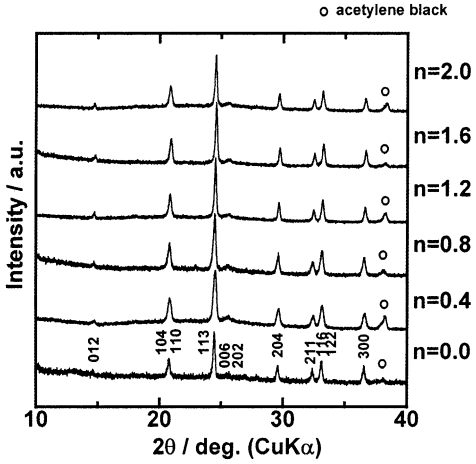

Fig. 6. XRD patterns of Mg inserted $Mg_{0.5+n/2}Ti_2(PO_4)_3$.

x_{lim} and $(1/j)$ at $|-j| = 50\ \mu A\ cm^{-2}$, suggesting that Mg insertion is controlled by the diffusion process.

3.3. Lithium insertion behaviors for comparison

Discharge curves of electrochemical Li^+ and Mg^{2+} insertion are compared in Fig. 5. The Li insertion proceeds in consists of several steps in contrast to the one-step Mg insertion. Thus, Mg insertion behaviors seem to be different from Li insertion although Li insertion into $Mg_{0.5}Ti_2(PO_4)_3$ has not been reported. As a whole, the plateau potential (i.e. the number of acceptable electrons per unit formula) for Li insertion (Li^+/Li corresponds to -3.72 V versus Ag^+/Ag) is slightly higher than that for Mg insertion (Mg dissolution on anodes occur at -2.20 V versus Ag^+/Ag), whereas the discharge capacity for Li insertion is smaller than that for Mg insertion.

Changes in XRD patterns induced by electrochemical Mg and Li insertion are shown in Figs. 6 and 7, respectively. As seen in Fig. 6, there appears no substantial change after Mg insertion up to $n = 2.0$, where n denotes the number of inserted electrons per formulae. After Li insertion at $n = 2.0$, on the contrary (1 0 4) and (1 1 0) peaks originally overlapped at $2\theta = 21^\circ$ split remarkably as well as the (2 1 1) and (1 1 6) peak couple at $2\theta = 33^\circ$.

The unit cell parameters after Mg and Li insertion are compared in Fig. 8. The electrochemical Mg insertion does not lead to the lattice expansion up to $n = 2.0$, whereas the same lattice expands in the a-direction almost linearly with the amount of inserted Li. It has been known that Mg^{2+} (0.086 nm), Li^+ (0.090 nm), Ti^{4+} (0.075 nm) and Ti^{3+} (0.081 nm) ions occupy six-coordinated sites in NASICON-lattice [12]. The a-axis expansion observed only for Li accommodation may hardly be explained by slight difference in ionic radii between Li^+ and Mg^{2+}. Rather, the strong polarization of small and divalent Mg^{2+} seems to suppress the lattice expansion caused by the reduction of Ti^{4+} to Ti^{3+}. Anyhow, the expansion-less accommodation of Mg in $Mg_{0.5}Ti_2(PO_4)_3$ NASICON host should be favorable for an insertion electrode employed in secondary cells.

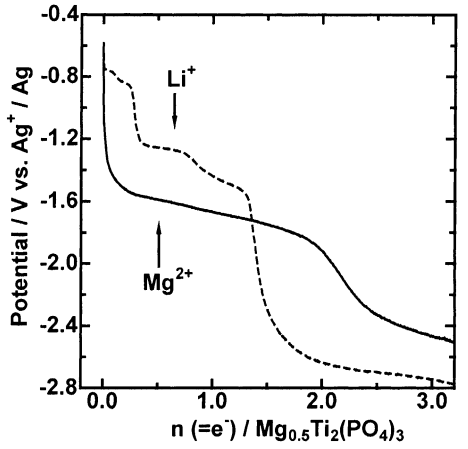

Fig. 5. Discharge curve for Li insertion compared with that for Mg insertion at $-50\ \mu A\ cm^{-2}$.

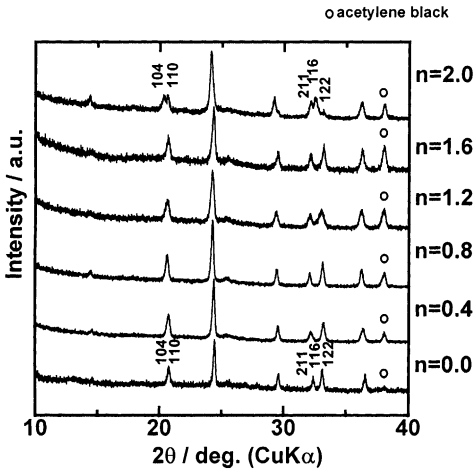

Fig. 7. XRD patterns of Li inserted $Li_nMg_{0.5}Ti_2(PO_4)_3$.

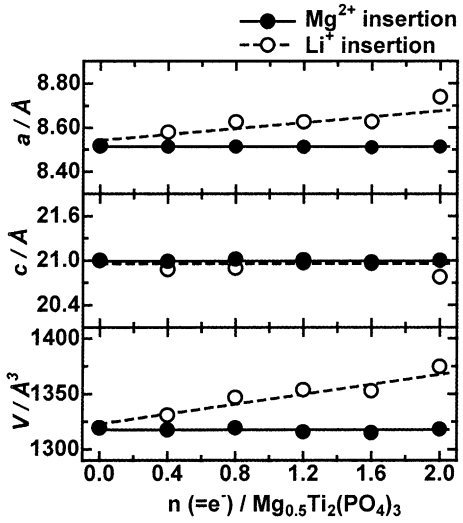

Fig. 8. Unit cell parameters at various stages of Mg and Li insertion.

4. Conclusion

Electrochemical magnesium insertion into $Mg_{0.5}Ti_2(PO_4)_3$ was found possible and one Mg^{2+} can be accommodated per unit formula. The slow diffusion of Mg in this host lattice requires another technological approach to reduce the time constant of diffusion. Mg^{2+} insertion could reduce the structural changes of the host compared with Li^+ insertion.

References

[1] P. Novák, W. Scheifele, O. Haas, J. Power Sources 54 (1995) 479.
[2] T.D. Gregory, R.J. Hoffman, R.C. Winterton, J. Electrochem. Soc. 137 (1990) 775.
[3] M.E. Spahr, P. Novák, O. Haas, R. Nesper, J. Power Sources 54 (1995) 346.
[4] P. Novák, W. Scheifele, F. Joho, O. Haas, J. Power Sources 142 (1995) 2544.
[5] P. Novák, J. Desilvestro, J. Electrochem. Soc. 140 (1993) 140.
[6] C. Delmas, A. Nadiri, Solid State Ionics 28 (1988) 419.
[7] C. Delmas, F. Cherkaoui, A. Nadiri, P. Hagenmuller, Mater. Res. Bull. 22 (1987) 631.
[8] C. Masquelier, A.K. Padhi, K.S. Nanjundaswamy, J.B. Goodenough, J. Solid State Chem. 135 (1998) 228.
[9] J.B. Goodenough, H.Y.P. Hong, J.A. Kafalas, Mater. Res. Bull. 11 (1976) 203.
[10] S. Barth, R. Olazcuaga, P. Gravereau, G. Le Flem, P. Hagenmuller, Mater. Lett. 16 (1993) 96.
[11] Y. Miyamoto, H. Takahashi, M. Kinoshita, A. Kishioka, J. Ceram. Soc., Jpn. 100 (1992) 1025.
[12] R.D. Shannon, Acta Crystallogr. A32 (1976) 751.